



A mixed finite-element formulation for the modal analysis of electromagnetic waveguides featuring improved low-frequency resolution of transmission line modes

R. Baltes¹, J. Al Ahmar², O. Farle¹, and R. Dyczij-Edlinger¹

¹Chair of Electromagnetic Theory, Dept. of Physics and Mechatronics, Saarland University, Saarbrücken, Germany

²Chair of Microintegration and Reliability, Dept. of Physics and Mechatronics, Saarland University, Saarbrücken, Germany

Correspondence to: R. Baltes (r.baltes@lte.uni-saarland.de)

Received: 25 January 2014 – Revised: 12 May 2014 – Accepted: 6 June 2014 – Published: 10 November 2014

Abstract. This paper presents an improved finite-element formulation for axially uniform electromagnetic waveguides. It allows for both dielectric and conduction losses and covers the entire range from optics down to the static limit. Propagation coefficients of small magnitude, particularly those of transmission line modes in the low-frequency regime, are computed much more accurately than with previous approaches.

1 Introduction

Since electromagnetic waveguides constitute generalized transmission line systems, they are of fundamental importance for the design of electromagnetic devices. Because of complex geometries and inhomogeneous materials, analytical solutions for the modal field patterns and propagation coefficients are often difficult to obtain or even unavailable. Numerical field simulation methods provide a powerful remedy. In particular the finite-element (FE) method stands out for its high convergence rates and great flexibility in modeling geometry and materials.

Early approaches suffered from the occurrence of spurious modes, but with the advent of $\mathcal{H}(\text{curl})$ conforming basis functions these problems were overcome. A great variety of FE formulations have been proposed: Some are in terms of the electric (Lee et al., 1991) or magnetic field intensity (Valor and Zapata, 1995), while others employ a magnetic vector potential and a electric scalar potential (Bardi and Biro, 1991; Polstyanko and Lee, 1995). They all provide accurate results for high frequencies, but very few can handle

the low-frequency (LF) (Vardapetyan and Demkowicz, 2003) or even the static case (Lee et al., 2003; Farle et al., 2004). Moreover, they incorporate electric conductivity σ by means of an equivalent imaginary part ε'' of the electric permittivity (Lee, 1994), which breaks down when the angular frequency ω tends to zero, due to

$$\varepsilon'' = \frac{\sigma}{\omega}. \quad (1)$$

All methods above lead to generalized algebraic eigenvalue problems for the square of the propagation coefficient. As will be detailed in Sect. 4.2, this strongly amplifies numerical round-off error in propagation coefficients of small magnitude, e.g. waveguide modes close to cut-off and, more importantly, transmission line (TEM or quasi-TEM) modes in the LF regime.

To overcome these limitations, we propose in Sect. 2 the prototype of a mixed-field formulation in terms of the electric field intensity \mathbf{E} and the magnetic flux density \mathbf{B} . Its distinguishing feature is that the sought eigenvalue is the propagation coefficient itself rather than its square. The suggested approach incorporates conduction losses quite naturally and minimizes round-off errors in propagation coefficients of small magnitude. In Sect. 3 we establish stability in the LF regime, by imposing suitable constraints.

The ability of a single formulation to predict the propagation characteristics of inhomogeneous transmission lines accurately from statics up to microwave frequencies is of great practical importance for mixed-signal analysis, particularly in the context of model-order reduction (Polstyanko et al., 1997; Bertazzi et al., 2002; Schultschik et al., 2008).

2 Formulation

We consider an axially uniform waveguide Ω pointing in the \hat{z} direction. Its boundary Γ , with unit outward normal vector $\hat{\mathbf{n}}$, is assumed to consist of perfect electric walls Γ_E and perfect magnetic walls Γ_H . Let Ω be connected and Γ_E non-empty. We denote the wavenumber, speed of light, and characteristic impedance, respectively, of free space by k_0 , c_0 , and η_0 . The relative magnetic permeability μ_r , the relative electric permittivity ε_r , and the electric conductivity σ are assumed to be scalar-valued. Thanks to uniformity along the waveguide axis, the modal fields are given by waves propagating in $\pm\hat{z}$ direction. For the negative \hat{z} direction, we have the decomposition (Pozar, 2005, p. 93)

$$\mathbf{E} = (\mathbf{E}_t + E_z \hat{z}) \exp(\gamma z), \quad (2)$$

$$\mathbf{B} = (\mathbf{B}_t + B_z \hat{z}) \exp(\gamma z), \quad (3)$$

where subscripts t and z denote transversal and longitudinal components, respectively, and γ is the propagation coefficient. Thus the differential operators ∂_z and ∇ simplify to

$$\partial_z = \gamma, \quad (4)$$

$$\nabla = \nabla_t + \partial_z \hat{z} = \nabla_t + \gamma \hat{z}. \quad (5)$$

By applying Eqs. (2)–(5) to Faraday's law and Ampere's law,

$$\nabla \times \mathbf{E} = -jk_0 c_0 \mathbf{B}, \quad (6)$$

$$\nabla \times \mu_r^{-1} c_0 \mathbf{B} = (jk_0 \varepsilon_r + \sigma \eta_0) \mathbf{E}, \quad (7)$$

we arrive at a homogeneous boundary value problem, given by the set of partial differential equations

$$\hat{z} \times (\gamma \mathbf{E}_t - \nabla_t E_z) = -jk_0 c_0 \mathbf{B}_t, \quad (8)$$

$$\hat{z} \cdot (\nabla_t \times \mathbf{E}_t) = -jk_0 c_0 B_z, \quad (9)$$

$$\hat{z} \times (\gamma \mu_r^{-1} c_0 \mathbf{B}_t - \nabla_t \mu_r^{-1} c_0 B_z) = (jk_0 \varepsilon_r + \sigma \eta_0) \mathbf{E}_t, \quad (10)$$

$$\hat{z} \cdot (\nabla_t \times \mu_r^{-1} c_0 \mathbf{B}_t) = (jk_0 \varepsilon_r + \sigma \eta_0) E_z, \quad (11)$$

subject to the boundary conditions

$$\left. \begin{array}{l} E_z = 0 \\ \hat{\mathbf{n}} \times \mathbf{E}_t = \mathbf{0} \\ \hat{\mathbf{n}} \cdot \mathbf{B}_t = 0 \end{array} \right\} \text{on } \Gamma_E, \quad (12)$$

$$\left. \begin{array}{l} \mu_r^{-1} B_z = 0 \\ \hat{\mathbf{n}} \times \mu_r^{-1} \mathbf{B}_t = \mathbf{0} \\ \hat{\mathbf{n}} \cdot \varepsilon_r \mathbf{E}_t = 0 \end{array} \right\} \text{on } \Gamma_H. \quad (13)$$

2.1 Finite-element representation

Let \mathcal{H}^1 , $\mathcal{H}^{\text{curl}}$, \mathcal{H}^{div} , and \mathcal{H}^0 denote the Sobolev spaces with respect to the operator in superscript (Boffi et al., 2013, pp. 4). We define the subspaces

$$\mathcal{H}_E^1 := \left\{ \lambda \in \mathcal{H}^1(\Omega) \mid \lambda = 0 \text{ on } \Gamma_E \right\}, \quad (14)$$

$$\mathcal{H}_E^{\text{curl}} := \left\{ \mathbf{u} \in \mathcal{H}^{\text{curl}}(\Omega) \mid \hat{\mathbf{n}} \times \mathbf{u} = \mathbf{0} \text{ on } \Gamma_E \right\}, \quad (15)$$

$$\mathcal{H}_E^{\text{div}} := \left\{ \mathbf{u} \in \mathcal{H}^{\text{div}}(\Omega) \mid \hat{\mathbf{n}} \cdot \mathbf{u} = 0 \text{ on } \Gamma_E \right\}, \quad (16)$$

and denote the corresponding finite-element spaces by $\mathcal{V}_E^1 \subset \mathcal{H}_E^1$, $\mathcal{V}_E^{\text{curl}} \subset \mathcal{H}_E^{\text{curl}}$, $\mathcal{V}_E^{\text{div}} \subset \mathcal{H}_E^{\text{div}}$, and $\mathcal{V}^0 \subset \mathcal{H}^0$. The transversal and axial fields $\mathbf{E}_t, E_z, \mathbf{B}_t, B_z$ are discretized by basis functions of lowest order (Zhu and Cangellaris, 2006, pp. 19), for their respective function spaces. Let N_N denote the number of free nodes, N_E the number of free edges, and N_F the number of faces in the mesh. Then

$$E_z = \sum_{k=1}^{N_N} x_{Ez,k} \lambda_k \quad \text{with } \lambda_k \in \mathcal{V}_E^1, \quad (17)$$

$$\mathbf{E}_t = \sum_{k=1}^{N_E} x_{Et,k} \mathbf{w}_k \quad \text{with } \mathbf{w}_k \in \mathcal{V}_E^{\text{curl}}, \quad (18)$$

$$c_0 B_z = \sum_{k=1}^{N_F} x_{Bz,k} W_k \quad \text{with } W_k \in \mathcal{V}^0, \quad (19)$$

$$c_0 \mathbf{B}_t = \sum_{k=1}^{N_E} x_{Bt,k} \mathbf{v}_k \quad \text{with } \mathbf{v}_k \in \mathcal{V}_E^{\text{div}}. \quad (20)$$

Note that Eqs. (19) and (20) have been scaled by c_0 , for numerical stability. The FE representations of the differential operators grad, curl, and div are given by the incidence matrices $\mathbf{G} \in \mathbb{R}^{N_E \times N_N}$, $\mathbf{R} \in \mathbb{R}^{N_F \times N_E}$, and $\mathbf{D} \in \mathbb{R}^{N_F \times N_E}$. Also, in two dimensions, we have (Zhu and Cangellaris, 2006, pp. 26)

$$\mathbf{D} = \mathbf{R}. \quad (21)$$

Since Eqs. (8) and (9) are in terms of fields represented on the primal mesh, they are discretized in strong form. In contrast, Eqs. (10) and (11) are based on the fields $\mathbf{H} = \mu^{-1} \mathbf{B}$, $\mathbf{D} = \varepsilon \mathbf{E}$, and $\mathbf{J} = \sigma \mathbf{E}$. These reside on the dual complex and are thus considered in weak form. The resulting generalized algebraic eigenvalue problem reads

$$(\mathbf{A} + jk_0 \mathbf{C}) \mathbf{x} = -\gamma \mathbf{B} \mathbf{x}. \quad (22)$$

At this point it can be seen that the eigenvalue is the propagation coefficient γ itself rather than its square. The vector and the matrices in Eq. (22) are given by

$$\mathbf{x} = \begin{bmatrix} x_{Bt} \\ x_{Bz} \\ x_{Et} \\ x_{Ez} \end{bmatrix}, \quad \mathbf{A} = \begin{bmatrix} \mathbf{0} & \mathbf{0} & \mathbf{0} & -\mathbf{G} \\ \mathbf{0} & \mathbf{0} & -\mathbf{R} & \mathbf{0} \\ \mathbf{0} & -\mathbf{R}^T \mathbf{T}_{Bz} & -\mathbf{T}_{\sigma t} & \mathbf{0} \\ \mathbf{G}^T \mathbf{T}_{Bt} & \mathbf{0} & \mathbf{0} & \mathbf{T}_{\sigma z} \end{bmatrix},$$

$$\mathbf{B} = \begin{bmatrix} \mathbf{0} & \mathbf{0} & \mathbf{I} & \mathbf{0} \\ \mathbf{0} & \mathbf{0} & \mathbf{0} & \mathbf{0} \\ -\mathbf{T}_{Bt} & \mathbf{0} & \mathbf{0} & \mathbf{0} \\ \mathbf{0} & \mathbf{0} & \mathbf{0} & \mathbf{0} \end{bmatrix}, \quad \mathbf{C} = \begin{bmatrix} \mathbf{I} & \mathbf{0} & \mathbf{0} & \mathbf{0} \\ \mathbf{0} & \mathbf{I} & \mathbf{0} & \mathbf{0} \\ \mathbf{0} & \mathbf{0} & -\mathbf{T}_{Et} & \mathbf{0} \\ \mathbf{0} & \mathbf{0} & \mathbf{0} & \mathbf{T}_{Ez} \end{bmatrix}, \quad (23)$$

where \mathbf{I} denotes the identity matrix. The other submatrices are defined as

$$T_{Bt,ij} = \int_{\Omega} \mathbf{v}_i \cdot \mu_r^{-1} \mathbf{v}_j \, d\Omega \quad \text{with } \mathbf{v}_i, \mathbf{v}_j \in \mathcal{V}_E^{\text{div}}, \quad (24)$$

$$T_{Bz,ij} = \int_{\Omega} W_i \mu_r^{-1} W_j \, d\Omega \quad \text{with } W_i, W_j \in \mathcal{V}^0, \quad (25)$$

$$T_{Et,ij} = \int_{\Omega} \mathbf{w}_i \cdot \varepsilon_r \mathbf{w}_j \, d\Omega \quad \text{with } \mathbf{w}_i, \mathbf{w}_j \in \mathcal{V}_E^{\text{curl}}, \quad (26)$$

$$T_{Ez,ij} = \int_{\Omega} \lambda_i \varepsilon_r \lambda_j \, d\Omega \quad \text{with } \lambda_i, \lambda_j \in \mathcal{V}_E^1, \quad (27)$$

$$T_{\sigma z,ij} = \eta_0 \int_{\Omega} \lambda_i \sigma \lambda_j \, d\Omega \quad \text{with } \lambda_i, \lambda_j \in \mathcal{V}_E^1, \quad (28)$$

$$T_{\sigma t,ij} = \eta_0 \int_{\Omega} \mathbf{w}_i \cdot \sigma \mathbf{w}_j \, d\Omega \quad \text{with } \mathbf{w}_i, \mathbf{w}_j \in \mathcal{V}_E^{\text{curl}}. \quad (29)$$

In absence of magnetic (dielectric) losses, we have $\mu_r \in \mathbb{R}^+$ ($\varepsilon_r \in \mathbb{R}^+$) everywhere, and the corresponding matrices \mathbf{T}_{Bt} and \mathbf{T}_{Bz} (\mathbf{T}_{Et} and \mathbf{T}_{Ez}) are positive definite. In contrast, $\mathbf{T}_{\sigma t}$ and $\mathbf{T}_{\sigma z}$ are positive semi-definite, because $\sigma > 0$ holds in the conductive region only.

3 Low-frequency behavior

For $k_0 = 0$, the eigenvalue problem of Eq. (22) reduces to

$$\mathbf{A}\mathbf{x} = -\gamma\mathbf{B}\mathbf{x}. \quad (30)$$

The matrix $\mathbf{A} + \gamma\mathbf{B}$ turns out to be singular, for any value of γ . We will analyze this effect and propose a suitable regularization.

3.1 Analysis of instability

We decompose the waveguide cross-section Ω into the lossless region Ω_{ll} , with $\sigma = 0$, the lossy subdomain Ω_l , with $\sigma > 0$, and their common interface Γ_0 :

$$\Omega = \Omega_l \cup \Omega_{ll} \cup \Gamma_0. \quad (31)$$

In view of Eq. (23), the eigenvalue problem for the static case, Eq. (30), is equivalent to

$$\gamma \mathbf{x}_{Et} = \mathbf{G} \mathbf{x}_{Ez}, \quad (32)$$

$$-\mathbf{R} \mathbf{x}_{Et} = \mathbf{0}, \quad (33)$$

$$\gamma \mathbf{T}_{Bt} \mathbf{x}_{Bt} + \mathbf{T}_{\sigma t} \mathbf{x}_{Et} = -\mathbf{R}^T \mathbf{T}_{Bz} \mathbf{x}_{Bz}, \quad (34)$$

$$\mathbf{G}^T \mathbf{T}_{Bt} \mathbf{x}_{Bt} + \mathbf{T}_{\sigma z} \mathbf{x}_{Ez} = \mathbf{0}. \quad (35)$$

Consider the vectors

$$\begin{bmatrix} \mathbf{x}_{Et,\gamma} \\ \mathbf{x}_{Ez,\gamma} \end{bmatrix} = \begin{bmatrix} \mathbf{G} \\ \gamma \mathbf{I} \end{bmatrix} \mathbf{x}_N, \quad (36)$$

$$\begin{bmatrix} \mathbf{x}_{Bt,\gamma} \\ \mathbf{x}_{Bz,\gamma} \end{bmatrix} = \begin{bmatrix} -\mathbf{T}_{Bt}^{-1} \mathbf{R}^T \mathbf{T}_{Bz} \\ \gamma \mathbf{I} \end{bmatrix} \mathbf{x}_F, \quad (37)$$

with $\mathbf{x}_F \in \mathbb{R}^{N_F}$ arbitrary and any $\mathbf{x}_N \in \mathbb{R}^{N_N}$ satisfying

$$x_{N,i} = \begin{cases} 0 & \text{if node } i \in \Omega_l \cup \Gamma_0, \\ \text{arbitrary} & \text{if node } i \in \Omega_{ll}. \end{cases} \quad (38)$$

Plugging Eqs. (36) and (37) into Eqs. (32)–(35) shows that these are satisfied for any arbitrary value of γ . The vectors

$$\mathbf{u}_\gamma = \begin{bmatrix} \mathbf{x}_{Bt,\gamma} \\ \mathbf{x}_{Bz,\gamma} \\ \mathbf{x}_{Et,\gamma} \\ \mathbf{x}_{Ez,\gamma} \end{bmatrix} \quad (39)$$

form the eigenspace corresponding to γ . To regularize the eigenvalue problem and eliminate the non-physical eigenvectors, we first analyze the vectors \mathbf{u}_γ . Let \mathbf{E}_γ and \mathbf{B}_γ denote the fields represented by Eqs. (36) and (37), respectively. In view of Eq. (38), \mathbf{E}_γ is nonzero in the lossless region only and, by Eq. (4), it is a gradient field. Similarly, it can be shown that the magnetic field strength \mathbf{H} corresponding to \mathbf{B}_γ is a gradient, represented on the dual mesh. Plugging \mathbf{E}_γ and \mathbf{B}_γ into Eqs. (6) and (7) and taking the divergence yields

$$-jk_0 c_0 \nabla \cdot \mathbf{B}_\gamma = 0, \quad (40)$$

$$jk_0 c_0^{-1} \nabla \cdot \varepsilon_r \mathbf{E}_\gamma = 0. \quad (41)$$

It can be seen that, for $k_0 = 0$, these fields are no longer forced to be source-free.

3.2 Stabilization

To stabilize the method, we impose the conditions

$$\nabla \cdot \mathbf{B} = 0 \quad \text{in } \Omega, \quad (42)$$

$$\nabla \cdot (\varepsilon_0 \varepsilon_r \mathbf{E}) = 0 \quad \text{in } \Omega_{ll}, \quad (43)$$

similarly to (Polstyanko et al., 1997; Hiptmair et al., 2008), by introducing Lagrange multipliers \mathbf{p}_F and \mathbf{p}_N . The discrete representations of Eqs. (42) and (43) read

$$\mathbf{D} \mathbf{x}_{Bt} + \gamma \mathbf{x}_{Bz} = \mathbf{R} \mathbf{x}_{Bt} + \gamma \mathbf{x}_{Bz} = \mathbf{0}, \quad (44)$$

$$\tilde{\mathbf{I}}_N \mathbf{G}^T \mathbf{T}_{Et} \mathbf{x}_{Et} - \gamma \tilde{\mathbf{I}}_N \mathbf{T}_{Ez} \mathbf{x}_{Ez} = \mathbf{0}, \quad (45)$$

where the matrix $\tilde{\mathbf{I}}_N$ selects the nodes belonging to the lossless regions Ω_{ll} .

Care must be taken if the structure is bounded by electric walls only ($\Gamma_H = \emptyset$). In this case, the transpose of the curl matrix \mathbf{R}^T , i.e. the gradient operator on the dual mesh, has a nontrivial nullspace of dimension one. It consists of constant fields and is represented by a coefficient vector \mathbf{x}_c with

$$x_{c,i} = \text{sign}(\det(\mathbf{J}_i)), \quad (46)$$

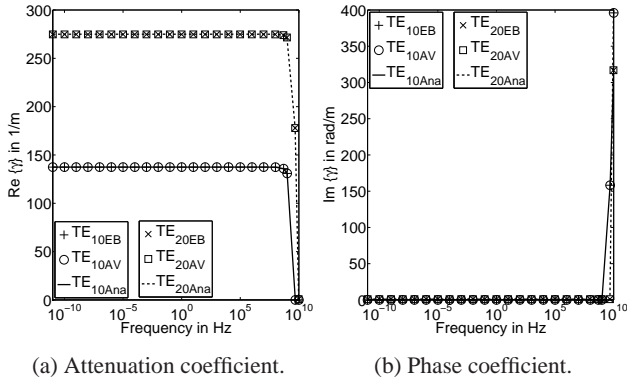


Figure 1. Lossless rectangular waveguide: propagation coefficients of TE₁₀ and TE₂₀ modes versus frequency.

where \mathbf{J}_i is the Jacobian matrix of face i . In view of Eq. (23), the corresponding kernel vector of \mathbf{A} reads

$$\mathbf{u}_c = \begin{bmatrix} \mathbf{0} \\ \mathbf{T}_{Bz}^{-1} \mathbf{x}_c \\ \mathbf{0} \\ \mathbf{0} \end{bmatrix}. \quad (47)$$

It is easy to verify that the fields of \mathbf{u}_c satisfy Eqs. (32)–(35) and (45). Moreover, Eq. (44) implies

$$\gamma(\mathbf{u}_c) = 0. \quad (48)$$

Thus there exists a zero eigenvalue corresponding to a constant magnetic field strength \mathbf{H} pointing in \hat{z} direction. To exclude the eigenpair ($\gamma = 0, \mathbf{x} = \mathbf{u}_c$), we impose the orthogonality constraint

$$\mathbf{x}_c^T \mathbf{x}_{Bz} = 0, \quad (49)$$

by introducing a Lagrange multiplier p_c . Thus, the stabilized eigenvalue problem for the case $\Gamma_H = \emptyset$ becomes

$$(\hat{\mathbf{A}} + jk_0 \hat{\mathbf{C}}) \hat{\mathbf{x}} = -\gamma \bar{\mathbf{B}} \hat{\mathbf{x}}, \quad (50)$$

with

$$\hat{\mathbf{A}} =$$

$$\begin{bmatrix} \mathbf{0} & \mathbf{0} & \mathbf{0} & -\mathbf{G} & \mathbf{0} & \mathbf{R}^T & \mathbf{0} \\ \mathbf{0} & \mathbf{0} & -\mathbf{R} & \mathbf{0} & \mathbf{0} & \mathbf{0} & \mathbf{x}_c \\ \mathbf{0} & -\mathbf{R}^T \mathbf{T}_{Bz} & -\mathbf{T}_{\sigma t} & \mathbf{0} & \mathbf{T}_{Et} \mathbf{G} \tilde{\mathbf{I}}_N^T & \mathbf{0} & \mathbf{0} \\ \mathbf{G}^T \mathbf{T}_{Bt} & \mathbf{0} & \mathbf{0} & \mathbf{T}_{\sigma z} & \mathbf{0} & \mathbf{0} & \mathbf{0} \\ \mathbf{0} & \mathbf{0} & \tilde{\mathbf{I}}_N \mathbf{G}^T \mathbf{T}_{Et} & \mathbf{0} & \mathbf{0} & \mathbf{0} & \mathbf{0} \\ \mathbf{R} & \mathbf{0} & \mathbf{0} & \mathbf{0} & \mathbf{0} & \mathbf{0} & \mathbf{0} \\ \mathbf{0} & \mathbf{x}_c^T & \mathbf{0} & \mathbf{0} & \mathbf{0} & \mathbf{0} & 0 \end{bmatrix},$$

$$\bar{\mathbf{B}} = \begin{bmatrix} \mathbf{0} & \mathbf{0} & \mathbf{I} & \mathbf{0} & \mathbf{0} & \mathbf{0} & \mathbf{0} \\ \mathbf{0} & \mathbf{0} & \mathbf{0} & \mathbf{0} & \mathbf{0} & \mathbf{I} & \mathbf{0} \\ -\mathbf{T}_{Bt} & \mathbf{0} & \mathbf{0} & \mathbf{0} & \mathbf{0} & \mathbf{0} & \mathbf{0} \\ \mathbf{0} & \mathbf{0} & \mathbf{0} & \mathbf{0} & -\mathbf{T}_{Ez} \tilde{\mathbf{I}}_N^T & \mathbf{0} & \mathbf{0} \\ \mathbf{0} & \mathbf{0} & \mathbf{0} & -\tilde{\mathbf{I}}_N \mathbf{T}_{Ez} & \mathbf{0} & \mathbf{0} & \mathbf{0} \\ \mathbf{0} & \mathbf{I} & \mathbf{0} & \mathbf{0} & \mathbf{0} & \mathbf{0} & \mathbf{0} \\ \mathbf{0} & \mathbf{0} & \mathbf{0} & \mathbf{0} & \mathbf{0} & \mathbf{0} & 0 \end{bmatrix},$$

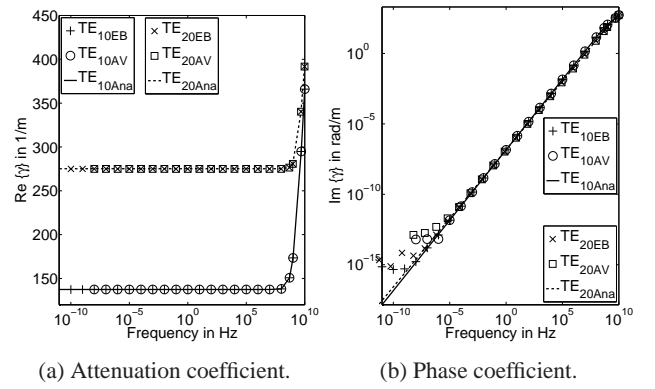


Figure 2. Lossy RWG with $\sigma = 5$ S/m: propagation coefficients of TE₁₀ and TE₂₀ modes versus frequency.

$$\hat{\mathbf{C}} = \begin{bmatrix} \mathbf{I} & \mathbf{0} & \mathbf{0} & \mathbf{0} & \mathbf{0} & \mathbf{0} & \mathbf{0} \\ \mathbf{0} & \mathbf{I} & \mathbf{0} & \mathbf{0} & \mathbf{0} & \mathbf{0} & \mathbf{0} \\ \mathbf{0} & \mathbf{0} & -\mathbf{T}_{Et} & \mathbf{0} & \mathbf{0} & \mathbf{0} & \mathbf{0} \\ \mathbf{0} & \mathbf{0} & \mathbf{0} & \mathbf{T}_{Ez} & \mathbf{0} & \mathbf{0} & \mathbf{0} \\ \mathbf{0} & \mathbf{0} & \mathbf{0} & \mathbf{0} & \mathbf{0} & \mathbf{0} & \mathbf{0} \\ \mathbf{0} & \mathbf{0} & \mathbf{0} & \mathbf{0} & \mathbf{0} & \mathbf{0} & \mathbf{0} \\ \mathbf{0} & \mathbf{0} & \mathbf{0} & \mathbf{0} & \mathbf{0} & \mathbf{0} & 0 \end{bmatrix}, \quad \hat{\mathbf{x}} = \begin{bmatrix} \mathbf{x}_{Bt} \\ \mathbf{x}_{Bz} \\ \mathbf{x}_{Et} \\ \mathbf{x}_{Ez} \\ \mathbf{p}_N \\ \mathbf{p}_F \\ \mathbf{p}_c \end{bmatrix}. \quad (51)$$

All eigenvectors of Eq. (50) that exhibit non-vanishing Lagrange multipliers, i.e. non-zero \mathbf{p}_N , \mathbf{p}_F or p_c , are known to span a subspace without physical meaning. This means the relevant subvectors do not solve the original eigenvalue problem Eq. (22). Rather than to purge such unwanted eigenvectors from the results, the authors prefer to shift the associated eigenvalues to infinity, so that they do not pollute the spectrum. This is easily accomplished, by setting the columns of $\bar{\mathbf{B}}$ that belong to Lagrange multipliers to zero. The modified matrix $\hat{\mathbf{B}}$ reads

$$\hat{\mathbf{B}} = \begin{bmatrix} \mathbf{0} & \mathbf{0} & \mathbf{I} & \mathbf{0} & \mathbf{0} & \mathbf{0} & \mathbf{0} \\ \mathbf{0} & \mathbf{0} & \mathbf{0} & \mathbf{0} & \mathbf{0} & \mathbf{0} & \mathbf{0} \\ -\mathbf{T}_{Bt} & \mathbf{0} & \mathbf{0} & \mathbf{0} & \mathbf{0} & \mathbf{0} & \mathbf{0} \\ \mathbf{0} & \mathbf{0} & \mathbf{0} & \mathbf{0} & \mathbf{0} & \mathbf{0} & \mathbf{0} \\ \mathbf{0} & \mathbf{0} & \mathbf{0} & -\tilde{\mathbf{I}}_N \mathbf{T}_{Ez} & \mathbf{0} & \mathbf{0} & \mathbf{0} \\ \mathbf{0} & \mathbf{I} & \mathbf{0} & \mathbf{0} & \mathbf{0} & \mathbf{0} & \mathbf{0} \\ \mathbf{0} & \mathbf{0} & \mathbf{0} & \mathbf{0} & \mathbf{0} & \mathbf{0} & 0 \end{bmatrix}, \quad (52)$$

and the final form of the eigenvalue problem is given by

$$(\hat{\mathbf{A}} + jk_0 \hat{\mathbf{C}}) \hat{\mathbf{x}} = -\gamma \hat{\mathbf{B}} \hat{\mathbf{x}}. \quad (53)$$

4 Numerical examples

4.1 Rectangular waveguide

We consider a rectangular waveguide (RWG) of dimensions 22.86 mm × 11.43 mm with perfectly conducting walls and homogenous material properties ($\epsilon_r = 4$, $\mu_r = 1$) in both the

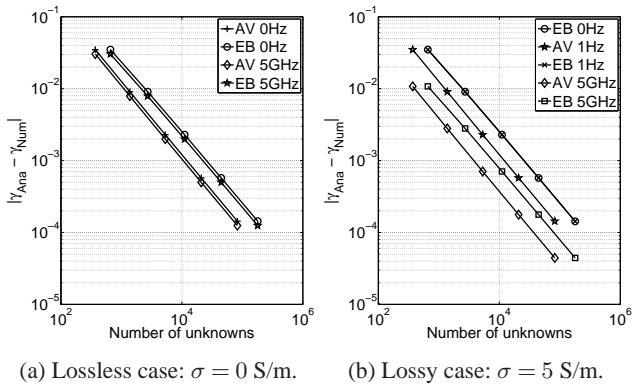


Figure 3. Convergence analysis for the TE₁₀ mode.

lossless case ($\sigma = 0$) and in presence of Ohmic losses ($\sigma = 5$ S/m). Our main goal is to demonstrate the correct function of the present approach and compare it to the $A - V$ potential formulation of (Farle et al., 2004), a state-of-the-art method that solves for γ^2 and models conductivity via complex permittivity, Eq. (1). According to (Pozar, 2005, p. 108), the analytical solution for the propagation coefficient γ_{mn} is given by

$$\gamma_{mn} = \sqrt{\left(\frac{m\pi}{a}\right)^2 + \left(\frac{n\pi}{b}\right)^2 - \epsilon_r \mu_r k_0^2 + j\mu_r \sigma k_0 \eta_0}, \quad (54)$$

where a and b denote the width and height of the waveguide, respectively. Figures 1 and 2 present the dispersion curves of the TE₁₀ and TE₂₀ modes in the frequency range $[10^{-10}, 10^{10}]$ Hz, and Fig. 3b gives the error in propagation coefficient as a function of the number of unknowns.

In the lossless case, the solutions of both the $E - B$ and $A - V$ methods are in very good agreement with the theory, over the whole frequency range; see Fig. 1. Figure 3a demonstrates that the convergence rates of both formulations are the same, for $f = 0$ Hz and $f = 5$ GHz, respectively.

In the lossy case ($\sigma = 5$ S/m), it can be seen from Fig. 2 that the $E - B$ approach works over the entire frequency range whereas the $A - V$ scheme fails to converge below 10^{-8} Hz, due to breakdown of Eq. (1). Above this threshold, the results of both methods agree very well with analytical results. The numerical noise visible in Fig. 2b for phase coefficients of very small magnitude, $\text{Im} \gamma < 10^{-12}$ rad/m, is insignificant because, as seen in Fig. 2a, the corresponding attenuation coefficients are more than 14 orders of magnitude larger, $\text{Re} \gamma > 120$. Figure 3b indicates that, within their respective range of validity, both numerical methods exhibit the same rate of convergence, independently of frequency. In case of the $E - B$ scheme, this also holds in the static case, $f = 0$ Hz.

4.2 Shielded microstrip line

The purpose of this example is to demonstrate the advantage of formulating the eigenvalue problem in terms of γ

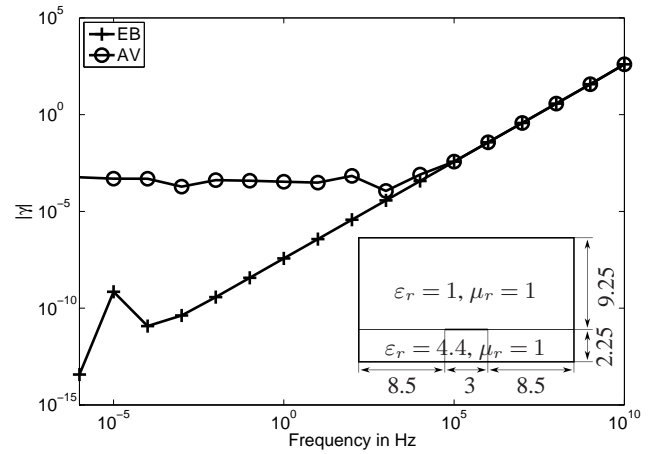


Figure 4. Shielded microstrip line: LF behavior of propagation coefficient of quasi-TEM mode. Inset shows cross-section of structure. Dimensions are in mm.

rather than γ^2 , with respect to round-off error in propagation coefficients of small magnitude. Again, we compare the $E - B$ and $A - V$ methods, by means of the lossless shielded microstrip line shown on the inset of Fig. 4. In contrast to the RWG of Sect. 4.1, the present structure supports a quasi-TEM mode, the phase coefficient of which is known to depend linearly on frequency in the LF regime. Figure 4 gives results for both numerical methods. While the $E - B$ data exhibit the expected behavior, the phase coefficients produced by the $A - V$ method stagnate for frequencies below 10^4 Hz. This may come as a surprise, because the latter formulation was designed to be low-frequency stable (Farle et al., 2004).

To clarify the situation, we present in Table 1 a comparison for not only the quasi-TEM wave but also the first two box modes. It can be seen that only the quasi-TEM mode is affected; the results for box modes are correct, even at 0 Hz. This behavior results from the fact that the static limit of $|\gamma|$ is zero for the quasi-TEM mode but non-zero for all others. At sufficiently low frequency values, $|\gamma_{\text{qTEM}}|$ becomes so much smaller than all other $|\gamma|$ values that the eigenvalue solver is unable to resolve γ_{qTEM} to sufficient accuracy, due to numerical noise. Note that the gap in eigenvalue $|\lambda_1/\lambda_2|$ is

$$\left| \frac{\lambda_1}{\lambda_2} \right| = \begin{cases} \left| \frac{\gamma_{\text{qTEM}}}{\gamma_{\text{Box } 1}} \right| & \text{for } E - B \text{ method,} \\ \left| \frac{\gamma_{\text{qTEM}}}{\gamma_{\text{Box } 1}} \right|^2 & \text{for } A - V \text{ method,} \end{cases} \quad (55)$$

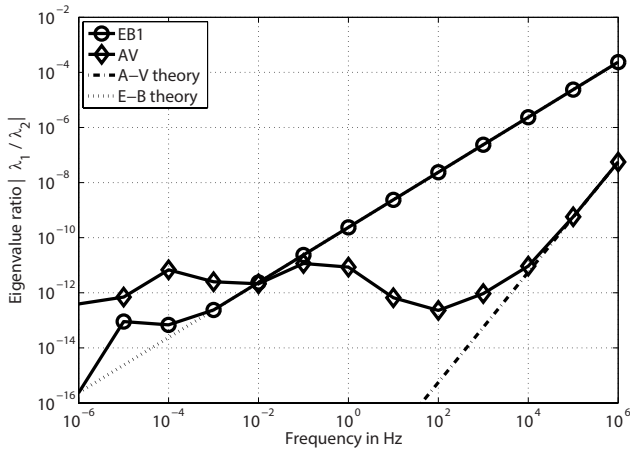
because the $E - B$ formulation solves for γ and the $A - V$ scheme for γ^2 . Figure 5 presents the eigenvalue ratio as a function of frequency. For both formulations, the eigenvalue solver produces significant round-off error for $|\lambda_1/\lambda_2| < 10^{-12} \dots 10^{-9}$. However, the frequency which this happens at is 10^4 Hz for the $A - V$ method, whereas the proposed $E - B$ scheme produces accurate results down to 10^{-3} Hz, thanks to improved eigenvalue ratio in Eq. (55).

Table 1. Comparison of first three modes of microstrip line.

Mode	Method	0 Hz	10 kHz	100 kHz
quasi-TEM	$E - B$	$1.6653e - 16$	$3.7160e - 04j$	$3.7162e - 03j$
	$A - V$	$4.7821e - 04j$	$8.6431e - 04$	$3.7630e - 03j$
Box 1	$E - B$	$1.5699e + 02$	$1.5699e + 02$	$1.5699e + 02$
	$A - V$	$1.5699e + 02$	$1.5699e + 02$	$1.5699e + 02$
Box 2	$E - B$	$2.6987e + 02$	$2.6987e + 02$	$2.6987e + 02$
	$A - V$	$2.6987e + 02$	$2.6987e + 02$	$2.6987e + 02$

Table 2. Computational data.

Example Method	Lossy RWG		Microstrip	
	$E - B$	$A - V$	$E - B$	$A - V$
Unknowns	11074	3969	13377	4416
Non-zeros $\hat{A} + \hat{C}$	73707	60167	107496	70602
Non-zeros \hat{B}	19844	34375	29328	39386
Runtime in sec	1.52	0.27	2.96	0.24
Iterations	85	59	82	55

**Figure 5.** Eigenvalue ratio versus frequency.

5 Critical discussion and conclusions

We have presented a mixed finite-element formulation for electromagnetic waveguides. Stability in the LF regime is achieved by imposing source-free conditions for the electric and magnetic flux densities, with the help of Lagrange multipliers.

Since the sought eigenvalue is the propagation coefficient itself rather than its square, round-off errors in propagation coefficients of small magnitude are significantly reduced. This is of great practical importance for the mixed-signal analysis of transversally inhomogeneous transmission line structures, such as microstrips or coplanar waveguides: For the example of Sect. 4.2, the LF range is extended by 7 orders of magnitude, compared to γ^2 approaches. Another feature of the proposed method is that Ohmic losses enter the formulation directly rather than in the form of equivalent complex permittivity.

The advantages of the new method do not come for free, though. Table 2 shows that the number of variables is three times as large as in the $A - V$ case. Nevertheless, the non-zeros in $\hat{A} + \hat{C}$ just increase by 50 %, and those in \hat{B} actually decrease. Iteration counts of the `eigs` solver of MATLAB-R2013a are 50 % higher for the $E - B$ approach. As a result, solution times for the lossy RWG are six times as long. For the microstrip, that ratio is twelve because, in the lossless

case, the system matrices of the $A - V$ method become real-valued, whereas those of the $E - B$ scheme remain complex.

Acknowledgements. This work was supported in part by grant DY 112/1-1 of the Deutsche Forschungsgemeinschaft (DFG).

Edited by: U. van Rienen

Reviewed by: two anonymous referees

References

- Bardi, I. and Biro, O.: An efficient finite-element formulation without spurious modes for anisotropic waveguides, *IEEE T. Microw. Theory*, 39, 1133–1139, 1991.
- Bertazzi, F., Peverini, O. A., Goano, M., Ghione, G., Orta, R., and Tascone, R.: A fast reduced-order model for the full-wave FEM analysis of lossy inhomogeneous anisotropic waveguides, *IEEE T. Microw. Theory*, 50, 2108–2114, 2002.
- Boffi, D., Brezzi, F., and Fortin, M.: *Mixed Finite Element Methods and Applications*, Springer, Berlin, 2013.
- Farle, O., Hill, V., and Dyczij-Edlinger, R.: Finite-Element Waveguide Solvers Revisited, *IEEE T. Magn.*, 40, 1468–1471, 2004.
- Hiptmair, R., Krämer, F., and Ostrowski, J.: A Robust Maxwell Formulation for All Frequencies, *IEEE T. Magn.*, 44, 682–685, 2008.
- Lee, J.-F.: Finite Element Analysis of Lossy Dielectric Waveguides, *IEEE T. Microw. Theory*, 42, 1025–1031, 1994.
- Lee, J.-F., Sun, D. K., and Cendes, Z. J.: Full-Wave Analysis of Dielectric Waveguides Using Tangential Vector Finite Elements, *IEEE T. Microw. Theory*, 39, 1262–1271, 1991.
- Lee, S.-C., Lee, J.-F., and Lee, R.: Hierarchical vector finite elements for analyzing waveguiding structures, *IEEE T. Microw. Theory*, 51, 1897–1905, 2003.
- Polstyanko, S. V. and Lee, J.-F.: $H_1(\text{curl})$ Tangential Vector Finite Element Method for Modeling Anisotropic Optical Fibers, *J. Lightwave Technol.*, 13, 2290–2295, 1995.
- Polstyanko, S. V., Dyczij-Edlinger, R., and Lee, J.-F.: Fast Frequency Sweep Technique for the Efficient Analysis of Dielectric Waveguides, *IEEE T. Microw. Theory*, 45, 1118–1126, 1997.
- Pozar, D. M.: *Microwave Engineering*, 3rd Edition, John Wiley & Sons, New York, 2005.
- Schultschik, A., Farle, O., and Dyczij-Edlinger, R.: A Model Order Reduction Method for the Finite-Element Simulation of Inhomogeneous Waveguides, *IEEE T. Magn.*, 44, 1394–1397, 2008.
- Valor, L. and Zapata, J.: Efficient Finite Element Analysis of Waveguides with Lossy Inhomogeneous Anisotropic Materials Char-

- acterized by Arbitrary Permittivity and Permeability Tensors, IEEE T. Microw. Theory, 43, 2452–2459, 1995.
- Vardapetyan, L. and Demkowicz, L.: Full-wave analysis of dielectric waveguides at a given frequency, Math. Comput., 72, 105–129, 2003.
- Zhu, Y. and Cangellaris, A. C.: Multigrid Finite Element Methods for Electromagnetic Field Modeling, IEEE Press, New Jersey, 2006.